Eur. Radiol. 10, 586–589 (2000)

European
Radiology

Case report

Xanthogranulomatous pyelonephritis: MRI findings in the diffuse and the focal type

G. Verswijvel[1], **R. Oyen**[1], **H. Van Poppel**[2], **T. Roskams**[3]

[1] Department of Radiology, University Hospitals Gasthuisberg, Catholic University of Leuven, Herestraat 49, B-3000 Leuven, Belgium
[2] Department of Urology, University Hospitals Gasthuisberg, Catholic University of Leuven, Herestraat 49, B-3000 Leuven, Belgium
[3] Department of Pathology, University Hospitals Gasthuisberg, Catholic University of Leuven, Herestraat 49, B-3000 Leuven, Belgium

Received: 15 February 1999; Revised: 14 June 1999; Accepted: 8 July 1999

Abstract. Two cases of xanthogranulomatous pyelonephritis (XGP) are presented with emphasis on MR appearances. One case is the diffuse type of XGP secondary to chronic obstruction caused by transitional cell carcinoma of the renal pelvis. The other case is the focal or "tumefactive" type of XGP which mimics renal cell carcinoma.

Key words: Kidney – Kidney inflammation – Genitourinary system – Xanthogranulomatous pyelonephritis – MR imaging

Introduction

Xanthogranulomatous pyelonephritis (XGP) is an uncommon type of chronic suppurative renal inflammation. It is characterised by destruction and replacement of the renal parenchyma by masses of lipid-containing macrophages. The inflammatory process may be focal or diffuse, can extend outside the kidney and can be complicated by fistula formation [1].

Although the macro-morphological changes, which occur in the diffuse type, are easily recognisable on imaging studies, diagnosis of the focal pseudo-tumoural type may be extremely difficult and unfortunately the lesion is often indistinguishable from a renal neoplasm.

Two cases of XGP are presented, both imaged with MR. The findings are correlated with the literature. Current radiological methods and an increased awareness of XGP should improve the ability to obtain the diagnosis of XGP preoperatively.

Correspondence to: R. Oyen

Case reports

Case 1

A 65-year-old male presented with fatigue, anorexia and intermittent dysuria. He had lost 14 kg of weight over a period of 2 months. He was a heavy cigarette smoker and had alcohol abuse. Clinical examination revealed a large palpable mass in the left flank. Blood biochemistry showed increased C-reactive protein (164 mg/l) and anaemia (haemoglobin 9.4 g/dl). Massive pyuria and haematuria was found on urinalysis. Urine culture revealed *E. coli*.

Abdominal US showed an enlarged left kidney with preservation of the renal outline and with large anechoic spaces scattered throughout the entire kidney. Prominent thickening of the wall of the dilated renal pelvis was present. The right adrenal gland was nodularly enlarged.

Computed tomography showed diffuse enlargement of the left kidney associated with perirenal stranding and perirenal fascial thickening. Multiple fluid-filled spaces throughout the kidney were seen, showing strong rim enhancement after intravenous contrast medium administration. There was no contrast medium excretion into the left pelvicalyceal system. The thickened wall of the left renal pelvis enhanced less than the borders of the intraparenchymal cavities. The right adrenal gland was enlarged; attenuation numbers precontrast were 20 Hounsfield units (HU).

Morphological features on MR imaging correlated well with the findings on CT. The fluid-containing cavities were hypointense on T1-weighted images and hyperintense on T2-weighted images. An intralocular fluid–fluid level was present in some of the cystic spaces (Fig. 1). The surrounding cavitary borders were slightly hyperintense on T1-weighted images (Fig. 2) and isointense on T2-weighted images compared with the parenchyma of the contralateral kidney. The thickened wall of the left renal pelvis was isointense on both T1- and T2-weighted images. After IV administration of gado-

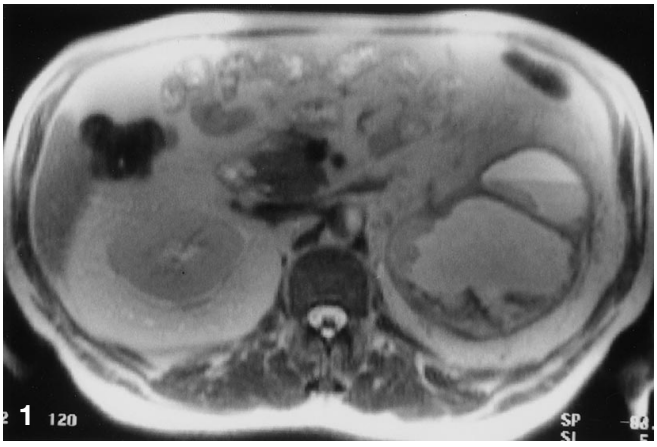

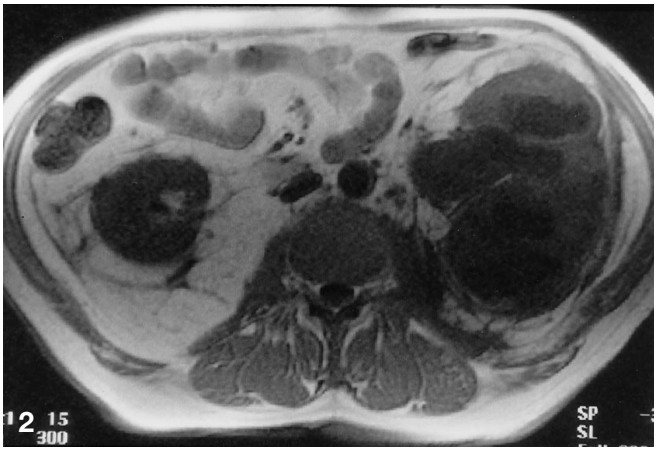

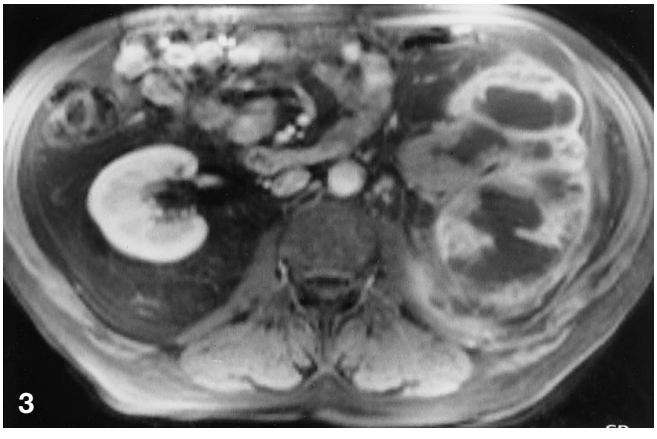

Fig. 1. A T2-weighted image (TR = 4.3 ms, TE = 60.0 ms). A fluid–fluid level is present in some of the cavities. Note the irregular outline of the internal margin of the large posterior cavity

Fig. 2. A T1-weighted image (TR = 7.7 ms, TE = 4.2 ms). Enlargement of the left kidney with multiple hypointense cavities. The pericavitary rims are hyperintense compared with the contralateral normal parenchyma. Hypointense perirenal fascial thickening is seen. Note the presence of hypointense tissue adjacent to the left psoas muscle. Some small para-aortic lymph nodes are present

Fig. 3. T1-weighted fat-saturated image after Gd-DTPA. Bright enhancement of the pericavitary rims is present representing inflammatory hyperaemia. Note enhancement of the perirenal fascial thickening as well of the perirenal inflammatory tissue adjacent to the psoas muscle. The thickened wall of the renal pelvis enhances to a lesser degree

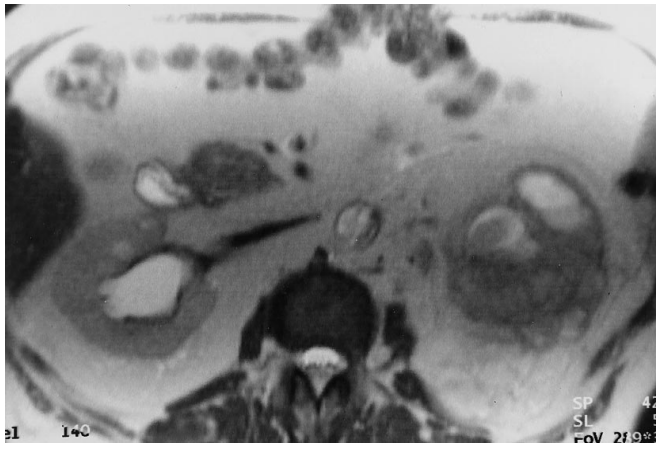

Fig. 4. T2-weighted image (TR = 4.3 ms, TE = 60.0 ms). Predominant isointense appearance of the tumefactive process in the left kidney. Some cavities contain a fluid–fluid level

linium dimeglumine (Gd-DTPA) the thickened pelvic wall enhanced less than the cavitary rims (Fig. 3). Prominent perirenal fascial thickening was present, hypointense on both T1-weighted and T2-weighted images and most prominent adjacent to the left psoas muscle (Figs. 1, 2). There was clear enhancement of the thickened perirenal fascia.

Left nephro-ureterectomy and right adrenalectomy were performed. Pathology revealed low-grade papillary transitional cell carcinoma of the renal pelvis with associated XGP. The renal parenchyma was replaced by large abscess formation. Histology revealed abundant lipid-laden macrophages (so-called xanthoma cells), lymphocytes and plasmocytes in the cavitary rims. The enlarged right adrenal gland was an adenoma.

Case 2

A 63-year-old male with a previous history of TCC of the bladder, treated with cystoprostatourethrectomy and a Mainz-pouch continent bladder reconstruction, presented with fever. Clinical examination showed tenderness in the left renal area. Blood biochemistry revealed anaemia (haemoglobin 9.1 g/dl) and an increase of creatinine level (1.62 mg/dl). Pyuria was seen on urine analysis and urine culture remained sterile.

Abdominal US showed bilateral dilatation of the collecting system. There was a heterogeneous predominant hypoechoic mass in the upper pole of the left kidney, containing multiple small cystic spaces.

On MR imaging the small cystic spaces of the upper pole mass were hypointense on T1-weighted images and hyperintense (but less than cerebrospinal fluid) on T2-weighted images. Some contained a fluid–fluid level (Fig. 4). The cavitary rims were isointense compared with the parenchyma of the contralateral kidney, on both T1- and T2-weighted images. Intravenous contrast medium was not given in this case.

A pouchogram did not show ureteral reflux. Ureterorenoscopy was normal. Left nephrectomy was per-

formed. Pathological examination revealed focal XGP. Small purulent foci were found and histology showed abundant xanthoma cells intermixed with lymphocytes and plasma cells.

The MR features of both cases are summarized in Table 1.

Table 1. Comparison of MRI findings in both cases

	Case 1 Diffuse XGP	Case 2 Focal XGP
T1-weighted		
Cavitary borders[a]	Hyperintense	Isointense
Cavitary fluid	Hypointense	Hypointense
Perirenal strands	Hypointense	Hypointense
T2-weighted		
Cavitary borders	Isointense	Isointense
Cavitary fluid	Hyperintense	Hyperintense
Perirenal strands	Hypointense	Hypointense
Fluid level	Present	Present
Gd-DTPA		
Cavitary borders	Enhancement	Not applicable
Cavitary fluid	No enhancement	
Perirenal strands	Enhancement	

[a] Compared with the contralateral (normal) renal parenchyma

Discussion

Both the focal and the diffuse type of XGP represent a chronic granulomatous nephritis with renal parenchymal destruction. Xanthogranulomatous pyelonephritis is a chronic cellular reaction with prominent lipid-laden histiocytes or macrophages, so called foam- or xanthoma cells [1].

Gross morphological changes include renal enlargement, peripelvic fibrosis, hydronephrosis and the presence of lobulated yellow masses replacing the normal renal parenchyma [2]. The renal cortical thickness is reduced and the cortex may contain multiple abscesses surrounded by xantoid tissue [1]. Xanthogranulomatous pyelonephritis most frequently results from chronic obstruction with chronic bacteriuria [1]. A large- or a staghorn calculus is found in up to 80% of cases. Association with TCC of the renal pelvis, as presented in the first case, is very rare, occurring in only 3.3% of cases [3]. Xanthogranulomatous pyelonephritis has been described in patients with ileal loop diversion with tumour recurrence [4]; however, no underlying obstruction was found in our second case.

In its most frequent type, XGP is diffuse and has fairly characteristic diagnostic imaging features. Less frequently renal involvement is focal and the mass lesion may mimic renal malignancy. Unfortunately, no pathognomonic radiological or clinical features exist to reliably differentiate focal XGP from renal cell carcinoma. However, if the clinical context is suggestive and radiology shows a mass with "atypical" features, in selected cases a trial with antibiotic therapy with careful imaging follow-up should be considered. Such a conservative approach can obviate nephrectomy [6].

There are few reports on MR characteristics of XGP. The morphological features of XGP are equally displayed by MR and CT [6, 9,10]. Reports on signal intensity characteristics of the XGP differ to some extent. Lipuma et al. [7], Jöerg et al. [8] and Laugareil et al. [9] described a hyperintense appearance of the solid component of XGP on T1-weighted images, compared with the renal parenchyma, similar to our first case. In the reports of Jöerg et al. [8] and Laugareil et al. [9] this hyperintensity was nearly equal to that of intra-abdominal fat. Other authors report a more isointense appearance of the solid component on T1-weighted images, as in the second case [6, 10, 11, 12]. It is probable that the signal intensity of the solid component of XGP on T1-weighted images depends on the amount of xanthoma cells involved in the granulomatous process.

The signal intensity on T2-weighted images was isointense in both cases, compared with the contralateral (normal) kidney, in agreement with the current literature on MR imaging of XGP [6, 7, 8, 9, 10, 11, 12]. The content of the "locular" spaces or cavities was hypointense on T1-weighted images and hyperintense on T2-weighted images in the cases presented, indicating a long T2. This too is in agreement with the descriptions in the literature [6, 7, 8, 9, 10, 11, 12]. Intracavitary fluid–fluid levels were observed on T2-weighted images in both cases, the upper part being hyperintense and the dependent part more hypointense. This reflects the heterogeneous composition of the content (e.g. fluid, debris, pus). The perirenal infiltration was hypointense on both T1- and T2-weighted images. According to Feldberg et al. this feature is inflammatory induced, or is due to the presence of thick fibrinous exudate [11].

Extensive reactive sinus replacement lipomatosis has been reported in XGP and is easily recognized and characterized with MR [9], but this feature was not seen in our cases. Strong rim enhancement of the borders of the cavities occurred after administration of Gd-DTPA, reflecting the associated hypervascularity of the inflamed tissue, but the collections themselves did not enhance. The thickened perirenal fascia also showed bright enhancement, reflecting true perirenal inflammatory extension. This finding, which is important for surgical planning, was better visualized on MR than on CT and has not been reported previously.

In conclusion, MR imaging has the ability to characterize and delineate diffuse and focal XGP and any perirenal extension.

References

1. Kenney PJ, Breathnach ES, Stanley RJ (1990) Chronic inflammation. In: Pollack HM (ed) Clinical urography. Saunders, Philadelphia, pp 827–835
2. Hayes WS, Hartman DS, Sesterbenn IA (1991) From the archives of the AFIP. Xanthogranulomatous pyelonephritis. Radiographics 11: 485–498
3. Val-Bernal JF, Castro F (1996) Xanthogranulomatous pyelonephritis associated with transitional cell carcinoma of the renal pelvis. Urol Int 57: 240–245

4. Spring DB, Moss AA (1984) Computed tomography of ileal loop urinary diversion in adults. J Comput Assist Tomogr 8: 866–870
5. Claes H, Vereecken R, Oyen R, Van Damme B (1987) Xanthogranulomatous pyelonephritis with emphasis on computerized tomography scan. Urology 29: 389–393
6. Ramboer K, Oyen R, Verellen S, Vermeersch S, Baert AL, Verberckmoes R (1997) Focal xanthogranulomatous pyelonephritis mimicking a renal tumor: CT- and MR-findings and evolution under therapy. Nephrol Dial Transplant 12: 1028–1030
7. Lipuma JP (1984) Magnetic resonance imaging of the kidney. Radiol Clin North Am 22: 925–941
8. Jöerg A, Cussenot O, Houlle D, Despoisse JM, Le Duc A (1989) La pyélonéphrite xanthogranulomateuse intérêt de l'imagerie par resonance magnétique. Ann Urol 23: 232–235
9. Laugareil P, Blery M, Despoisse, Changnon S (1989) Pyélonéphrite xanthogranulomateuse avec prolifération graisseuse de la loge renale. Aspects en tomodensitométrie et IRM. J Radiol 70: 295–297
10. Mulopulos GP, Patel SK, Pessis D (1986) MR imaging of xanthogranulomatous pyelonephrits. J Comput Assist Tomogr 10: 154–156
11. Feldberg MA, Driessen LP, Witkamp TD, van Leeuwen MS, van Waes PFG (1988) Xanthogranulomatous pyelonephritis: comparison of extent using computed tomography and magnetic resonance imaging in one case. Urol Radiol 10: 92–94
12. Hadley MD, Nichols DM, Smith FW (1982) Nuclear magnetic resonance tomographic imaging in xanthogranulomatous pyelonephritis. J Urol 127: 301–303